Applied Ocean Research 30 (2008) 144–152

Contents lists available at ScienceDirect

Applied Ocean Research

journal homepage: www.elsevier.com/locate/apor

Maximum wave crest and height statistics of irregular and abnormal waves in an offshore basin

P. Petrova, C. Guedes Soares *

Centre for Marine Technology and Engineering (CENTEC), Technical University of Lisbon, Instituto Superior Técnico, Lisboa, Portugal

ARTICLE INFO

Article history:
Received 12 January 2008
Received in revised form
4 August 2008
Accepted 12 August 2008
Available online 21 September 2008

Keywords:
Abnormal waves
Rogue waves
Freak waves
Wave statistics
Second order wave theory

ABSTRACT

Irregular deep water sea states generated in a tank and represented by a JONSWAP spectrum have been investigated with respect to the statistics of the largest waves. The crests and heights of the maximum observed waves have been fitted by linear and second order statistical models. Special attention has been given to the extreme waves, which fulfil simultaneously the criteria for the crest and height abnormality indices. Statistically, the non-Gaussian behaviour of the considered wave fields has been demonstrated by means of the coefficients of skewness and kurtosis estimated from the time series. The estimates have been compared with second order theory. Moreover, analytical formulae taking into account the effects of spectral bandwidth and finite depth have been applied to improve the predictions of the normalized cumulants. The obtained results showed that the largest crests are well described by the models with correction of third order included, by means of the coefficient of kurtosis. The maximum wave heights and the observed abnormal extremes agree well with the second-order theory, although the linear predictions do not deviate much from the observations either. The laboratory results are compared with results for full-scale data gathered during a storm at the North Alwyn platform in the North Sea. The storm data show different statistical behaviour.

1. Introduction

Much interest has been directed recently towards the study of the so called abnormal, freak or rogue waves. Several examples of abnormal waves measured at sea have appeared in the literature [41,42,24,33,9,19,20]. However, the lack of a complete understanding of rogue wave events explains the various definitions and theories for the physical mechanisms giving rise to these extremely large and steep waves.

The occurrence of abnormal waves is generally attributed to three possible mechanisms: the linear interaction between waves and currents [51]; the linear superposition of the Fourier random phases [27] and the modulation instability in random wave trains on deep water [49,37]. Other approaches based on wave focusing in model basins are due to Clauss [10] and Bateman et al. [4]. The sea state directionality, expressed in the superposition of two wave systems propagating in different direction [18] could be also an explanation for the generation mechanism of rogue waves, as suggested by Donelan and Magnusson [12].

Besides the scientific aspect of understanding the phenomenon, the practical application in the design and safe operation of ships and offshore structures is of primary importance, as discussed by Faulkner and Buckley [13], Fonseca et al. [16], Haver [25], Guedes Soares et al. [21]. In this respect, controlled model tests in a laboratory could be useful in studying the characteristics of waves that are rarely encountered at sea and the corresponding response of marine structures. Consequently, they can be applied to validate the calculations performed in the design practice.

Ship and offshore model basins have been in operation for many years and have been shown to be able to reproduce well the characteristics of sea waves in model scale and thus have been used successfully to study the behaviour of ships and offshore structures. The study of the design conditions requires the generation of extreme waves, which have been reproduced in laboratory experiments with generated 2D deep water waves, for example by Stansberg [43] and Mori and Yasuda [32].

However, while wave properties in model basins have been extensively checked, the characteristics of laboratory generated extreme and abnormal waves still require verification [45]. This is the motivation of the present paper, which makes part of a study on the behaviour of irregular waves generated in offshore basins [38,2].

The crests and heights of the maximum observed waves have been fitted by available linear and second order statistical models [46,45,52] with special attention paid to the abnormal wave events. The second order correction in the model of the surface elevation introduces the wave steepness, thus increasing the maximum predicted crest height, due to the nonlinearity of steep waves.

* Corresponding author. Tel.: +351 218417957.
E-mail address: guedess@mar.ist.utl.pt (C. Guedes Soares).

0141-1187/$ – see front matter © 2008 Elsevier Ltd. All rights reserved.
doi:10.1016/j.apor.2008.08.004

As discussed by Haver [25], the second order approximation is considered in the offshore industry as the most elaborated wave theory for design purposes, as far as it reasonably represents field measurements [17], as well as laboratory waves [45]. Probability distributions of narrow-band second order wave crests were given first by Tayfun [46]. Al-Humoud et al. [1] derived analytical expressions applicable to the wave amplitude statistics of a weakly nonlinear random sea, based on the concept of wave envelope and phase and without restrictions on the spectral bandwidth or wave directionality. The more general model of Arena and Fedele [3] defines the statistical properties of a family of second-order narrow-band random processes. Elaborated expressions for the crest height statistics for an arbitrary spectrum have been obtained by Fedele and Arena [14], extending Boccotti's quasi-determinism theory of the highest waves [8] to second order. The latter model demonstrated good agreement with both simulated and experimental data, including abnormal wave events. Other generalizations are due to Forristall [17] for 2D and 3D waves propagating at any depth.

However, the second order model underestimates significantly the extreme wave crests of field data, as discussed by Petrova et al. [39,40]. Similar conclusions were obtained by Jha and Winterstein [26] for laboratory experiments and by Bitner-Gregersen and Hagen [7] for numerically reproduced second order waves. The effect of third order nonlinearities on the statistics of large crests have been considered in the distribution of Fedele and Tayfun [15] based on the concept of stochastic wave groups. Recently, Tayfun and Fedele [47] proposed slightly different expression based on the Gram–Charlier model for the distributions of the non-linear wave envelopes and phases.

The field data and numerical simulations analyzed so far have shown that the largest wave heights are usually overpredicted by the Rayleigh distribution mainly due to the finite spectral bandwidth and not to bound waves' effects [35,8]. Furthermore, it has been shown that the second order nonlinear correction could not affect noticeably the crest-to-trough wave height of the narrow-band waves, particularly the largest waves, which behave as if having a narrow-band spectrum [46,47]. Thus, the probabilistic models initially derived for waves with a narrow spectrum could also successfully represent the random sea waves, except for the extreme tail of the empirical distributions. Consequently, the adequate prediction of unexpectedly large wave heights should be pursued beyond the limits of the second order theory [25].

The deviation from the nonlinear, non-Gaussian statistics could be also attributed to Benjamin–Feir modulational instability in the wave train, which can be considered as a quasi-resonant four-wave interaction [36]. It has been shown in a series of studies with full-scale data [19], laboratory measurements [31,34] and numerical simulations (e.g. [32]) that the third order wave–wave interactions, expressed quantitatively by the coefficient of kurtosis, are responsible for the large-amplitude events and increase the probability of occurrence of freak waves. The coefficient of kurtosis was found to be in quadratic dependence with the Benjamin–Feir index, represented as the ratio between the wave steepness and the spectral bandwidth [34].

With respect to the coefficient of kurtosis, the second order approximation was reported to be more successfully applied to field data, than to waves in a tank, due to the fact that it tends to underestimate the high kurtosis values. Additionally, it is expected that the effect of kurtosis in the wind wave seas will be reduced, due to their short-crested nature. This explains the results reported by Jha and Winterstein [26], showing that the largest crest-to-trough wave heights in a tank tend to the Rayleigh statistics, while storm wave heights are well fitted by probabilistic models with included correction for the spectral bandwidth.

The identification of the waves as abnormal, freak or rogue is made according to a criterion that has not gained wide acceptance. Dean [11] studied 20-min time series and related them with the Rayleigh statistics, proposing an abnormality (amplification) index $AI = H_{max}/H_s > 2$. The designation H_{max} stands for the maximum wave height and H_s denotes the significant wave height calculated either from the spectrum or from the time series. Other authors considered the crest amplification index, $CI = C_{max}/H_s > R$, where C_{max} is the maximum wave height and R is some critical value. For example, Haver and Andersen [24] use $R = 1.2$. Tomita and Kawamura [48] apply the combination between $C_{max}/H_s > 1.3$ and $H_{max}/H_s > 2$, in order to define what they called 'genuine freak waves' and Clauss [10] used simultaneously $H_{max} \geq 2.15\,H_s$ and $C_{max} \geq 0.6\,H_{max}$.

The genuine freak wave's definition of Tomita and Kawamura [48] is the one adopted in the present study. Furthermore, the abnormality index AI should be exceeded by both down-crossing and up-crossing waves [19,20].

Although currently in use, the proposed criteria need further clarification. On one hand, they change when higher order approximation for the surface profile is assumed, since the nonlinearity increases the wave steepness, maximum crest and wave heights in comparison with the linear theory. Furthermore, the abnormal wave definitions are related to the record duration in a way that longer time series increase the probability of encountering an abnormal wave [11,6]. Also, the ratio depends on the choice of wave definition and on the way the significant wave height is calculated [19,20].

The present study aims at investigating the statistics of the maximum waves and the special cases of abnormal waves. The presence of extremely large wave events should contribute to significant deviations from the Gaussian surface model and the Rayleigh statistics. The obtained results for the waves generated in the offshore basin are compared with full-scale results based on storm data gathered at the North Alwyn platform in the North Sea.

The description of the applied analytical formulae for the extreme statistics is given first. Subsequently, the data are described, followed by discussion on the obtained results and the derived conclusions.

2. Statistical models

Statistical models, based on the linear and second order representation for the free surface are used, in order to predict the expected maxima of the modelled wave crests and heights.

Additionally, the third and fourth order normalized cumulants – the coefficient of skewness, γ_3, and the coefficient of kurtosis, γ_4, are used to measure the deviation from the Gaussian process. They are given as $\gamma_3 = \mu 3/\mu_2^{3/2}$ and $\gamma_4 = \mu_4/\mu_2^{4/2} - 3$, where μ_i denotes the ith central moment. In particular, the second order central moment $\mu_2 = \sigma^2$ shows the variance of the sea surface elevations. Quantitatively, γ_3 reflects the Stokian asymmetry in the wave profile and γ_4 represents the total increase of the crest-to-trough amplitude.

For a Gaussian random wave process, the extreme value distribution is given by Gumbel [23]. Subsequently, the expected maximum is expressed as a function of the number of independent crests, M, in the time series:

$$A_{1\,max} = E\,[A_{max}] = \sigma\left[\sqrt{2\ln(M)} + 0.5774/\sqrt{2\ln(M)}\right] \quad (1)$$

$$H_{1\,max} = E\,[H_{max}] = 2A_{1\,max} \quad (2)$$

where $A_{1\,max}$ is the linear maximum crest; $E[..]$ denotes statistical average; σ is the standard deviation of the free surface process and the factor 0.5774 is the Euler constant. The number of independent amplitudes, M, is obtained as the ratio between the duration of

the record, T, and the mean zero-up-crossing period, T_z, estimated from the spectral jth order moments m_j, $T_z = \sqrt{m_0/m_2}$. The expected largest linear wave height, $H_{1\max}$, is simply represented as twice the linear maximum $A_{1\max}$ Eq. (2).

Usually, the second order wave models describe adequately the real sea [17]. The non-linear effects increase significantly the crest height [29], which is reflected in the increased coefficient of skewness. On the other hand, the largest wave heights observed in heavy storms generally follow the Rayleigh distribution, due to the fact that the second order non-linear effects amplify the wave crests to the same extent as the wave troughs are decreased [46]. In this case, the coefficient of kurtosis is found to be the representative statistical measure for the increase in the total peak-to-trough height and is further related to the probability of occurrence of abnormal waves [30].

The second order extremes follow the theory of Tayfun [46]. The nonlinear terms in the proposed expressions reflect the contribution of wave steepness, given as $k_pA_{1\max}$, with k_p being the wave number, corresponding to the spectral peak period, T_p and $A_{1\max}$ being the linear amplitude from Eq. (1):

$$A_S = A_{1\max}\left(1 + \frac{1}{2}k_pA_{1\max}\right). \tag{3}$$

The applications of the second order approximation to field and laboratory data [28,29,43] or to data from numerical simulations [44] show general agreement.

Furthermore, the third order effects introduced by γ_4 in the nonlinear models account for the high and steep wave conditions. The formulae for the largest crest and wave heights with included γ_4 correction are empirically derived in the form [45]:

$$\frac{A_{St\max}}{\sigma} = \frac{A_{1\max}}{\sigma}\left(1 + \frac{\omega_p^2}{2g}A_{1\max}\right) + 1.3\gamma_4 \tag{4}$$

$$\frac{H_{St\max}}{2\sigma} = \frac{H_{1\max}}{2\sigma} + (\gamma_4 - 0.25). \tag{5}$$

Winterstein [52] proposed a more general representation for the observed crests and height extremes based on the Hermite transformation model. The model expands the non-Gaussian process $\eta(t)$ as a cubic function of the normalized Gaussian random process, $U(t)$:

$$\eta - \bar{\eta} = g(U) = k\sigma(U + c_3(U^2 - 1) + c_4(U^3 - 3U)). \tag{6}$$

Inputs to the representation in Eq. (6) are the first four statistical moments: mean ($\bar{\eta}$), standard deviation (σ), coefficient of skewness (γ_3) and coefficient of kurtosis (γ_4), estimated from the available records. The mean is set to zero. The third and fourth order statistics enter into the model by the set of non-dimensional coefficients: c_3, c_4 and k:

$$c_3 = \frac{\gamma_3}{6(1 + 6c_4)} \tag{7}$$

$$c_4 = \frac{\sqrt{1 + 1.5\gamma_4} - 1}{18} \tag{8}$$

$$k = \frac{1}{\sqrt{1 + 2c_3^2 + 6c_4^2}}. \tag{9}$$

Eq. (6) not only represents the nonlinear elevation process, but can be also used to estimate the extreme statistics of wave crests and heights. In particular, the extreme wave crest is given by the expression:

$$A_W = k\sigma\left[\frac{A_{1\max}}{\sigma} + c_3\left(\left(\frac{A_{1\max}}{\sigma}\right)^2 - 1\right) + c_4\left(\left(\frac{A_{1\max}}{\sigma}\right)^3 - 3\frac{A_{1\max}}{\sigma}\right)\right] \tag{10}$$

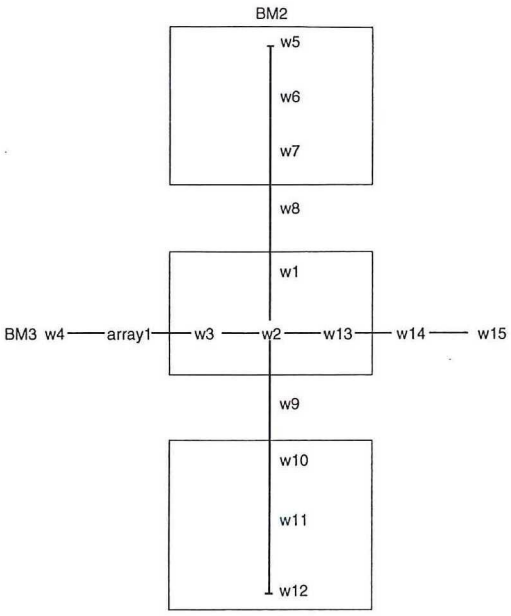

Fig. 1. Location of the wave gauges and the wave generators in the basin.

with $A_{1\max}$ being the linear crest from Eq. (1).

3. Data description and analysis of the results

The analyzed records represent measurements of the free surface elevation gathered at the offshore basin of MARINTEK. They span approximately 3 h 17 min and are sampled at $dt = 0.1768$ s. The surface oscillations are produced by two wave-makers: a double-flap wave-maker (BM2), installed at one of the short walls of the basin and a multiflap wave-maker (BM3), installed at one of the long sides of the basin (Fig. 1). The recordings are performed by 15 gauges, located as shown in Fig. 1. The experimental conditions describe deep water irregular unidirectional waves propagating on water of constant depth $d = 100$ m.

Two types of sea states have been considered (Table 1). The single sea states are defined by unimodal JONSWAP spectra with peakedness parameter $\gamma = 3$ and a combination of different peak periods, T_p and significant wave heights, H_s. The combined sea states consist of two wave systems propagating at an angle of 60°, 90° and 120°, represented by a bimodal JONSWAP spectrum with $\gamma = 3$ [18], $H_s = 3.6$ m and $T_p = 7$ s for the high-frequency spectral component and $H_s = 3.6$ m and $T_p = 20$ s for the low-frequency spectral component. The basic sea state parameters are described in Table 1. The wave energy is absorbed by a beach at the end of the tank opposite to BM2.

The generated wave fields have been checked for spatial variability by Petrova and Guedes Soares [38]. The non-parametric and parametric statistical tests applied have shown that the wave conditions of the unimodal seas can be considered statistically uniform throughout the basin. It has been also concluded that the higher sea states reflect increased consistency in the wave field. In the bimodal sea states, on the other hand, statistically significant differences have been observed, which led to the conclusion that special attention should be paid when such type of wave fields are generated. The largest spatial consistency for the directional sea states pertains to test 8235 with two wave systems propagating perpendicularly to each other (Table 1). The regions of consistency for the sea states with two wave systems were only demonstrated within the rectangles shown in Fig. 1. Three regions have been distinguished in that case.

Furthermore, the stationarity of the time series has also been validated using a non-parametric run-test described by Bendat

Table 1
Deep water irregular waves, $h = 100$ m

	Test no	Hs (m)	Tp (s)	Spectrum	Wave dir θ (deg)	Current velocity Uc (m/s)	Wave-maker
Unimodal	8201	3.5	10.0	J3	0	–	BM2
	8202	7.0	10.0	J3	0	–	BM2
	8219	9.0	10.0	J3	0	–	BM2
	8241	3.5	7.0	J3	0	–	BM2
Bimodal	8233	3.6/3.6	7.0/20.0	2P J3/J3	0/60	–	BM2/BM3
	8234	3.6/3.6	7.0/20.0	2P J3/J3	0/120	–	BM2/BM3
	8235	3.6/3.6	7.0/20.0	2P J3/J3	0/90	–	BM2/BM3

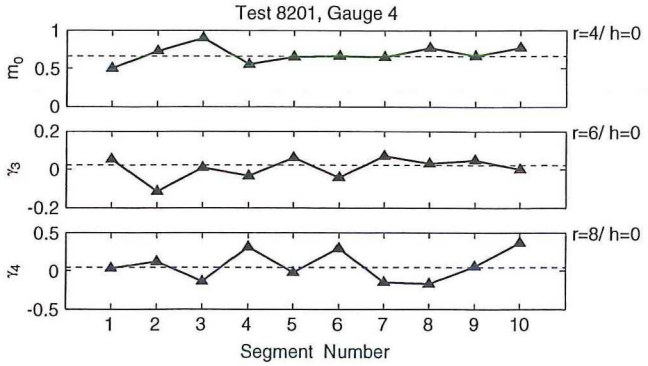

Fig. 2. Example of a run-test verifying the stationary conditions in the deep water records (according to Petrova and Guedes Soares [38]).

and Piersol [5]. The stationary condition is required, as it allows increasing the reliability of the estimates by using the entire record in the statistical analysis. The original time series have been split into $N = 10$ segments of approximately 20-min duration and the associated statistics have been estimated and compared with the corresponding median values.

Fig. 2 shows examples of the run-tests performed with respect to the zero-spectral moment, m_0, the coefficient of skewness, γ_3, and the coefficient of kurtosis, γ_4. The parameter r included in the figure denotes the number of consecutive runs of identical observations, as defined by Bendat and Piersol [5]. The region where the hypothesis should be accepted is determined as $r_{\frac{N}{2},1-\frac{\alpha}{2}} < r \leq r_{\frac{N}{2},\frac{\alpha}{2}}$, where α stands for the chosen level of significance. The lower bound of the critical interval for $N = 10$ and $\alpha = 0.05$ is determined as $r_{5,0.975} = 2$ and the upper limit as $r_{5,0.025} = 9$ (Table A.6 in [5]). Hence, the hypothesis of stationarity has to be rejected if the number of runs is less than 2 or more than 9. However, no significant results have been observed in any of the run tests performed, which is expressed by $h = 0$ in Fig. 2.

Following the zero-down-crossing definition, the mean number of waves found in each of the 3-h records varies from approximately $N = 1270$ for the severest sea state, designated by 8219, to $N = 1800$ waves for the lowest unidirectional sea with period $T_p = 7$ s designated by 8241 (Table 1).

The statistics of the largest crest heights have been considered, provided that the maximum wave crest is the one associated with the maximum wave in the record. In Fig. 3(a)–(c) the observed crest maxima are compared with the theoretical expectations, calculated from Eqs. (1)–(10). The solid line in the figures, designated as 'Perfect Fit' refers to the case when the maxima are perfectly fit by any of the models. The linear model is represented by diamond signs; the second order model is given by squares; the modified second order model of Stansberg [45] is given by triangles and the Hermite model's predictions [52] are represented by circles. The linear regression lines associated with the models are also drawn in the figures. It can be seen in Fig. 3(a)–(c) that the lowest crests up to approximately 7 m height are well predicted even by the linear model, which, however, underpredicts the higher waves. At the highest observed events the second order

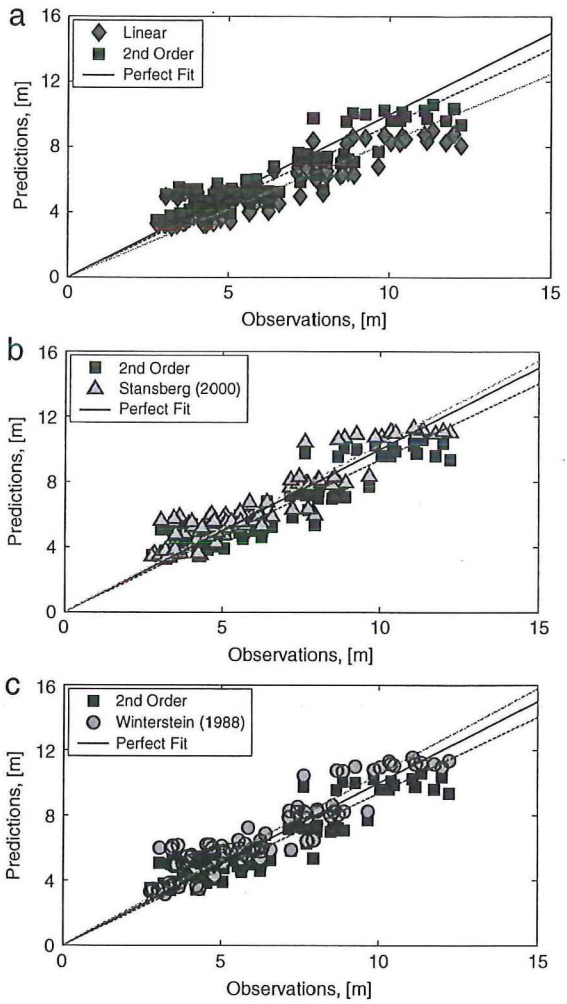

Fig. 3. Observed crest maxima in the offshore basin versus the theory: (a) linear model – second order model; (b) second order model – modified second order model of Stansberg; (c) second order model – modified second order model of Winterstein.

model and its modifications perform better. The second order model is found to increase the predictions of the linear model with 11%; the model of Stansberg gives almost 22% larger values and the Hermite transformation model shows 25% larger maximum crests, again compared to the linear statistics. It is seen that the modified second order models produce similar estimates for the expected extremes and consequently can be considered as being good approximations to the data for all sea states.

Considering separately the unimodal sea states, which have the same peak period of 10 s, it is possible to follow up the effect of wave steepness on the nonlinear crest statistics. For that purpose, the sea state steepness $S_p = H_s/L_p$ has been recalculated on the basis of the input significant wave height and the length of the harmonic corresponding to the input peak period. Thus, the three

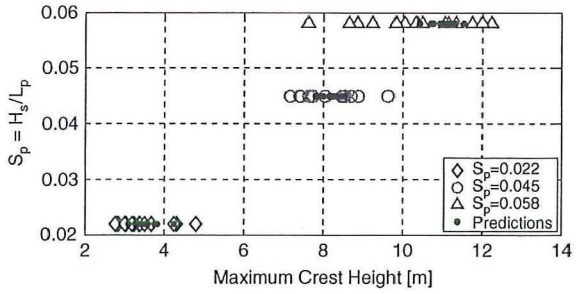

Fig. 4. Observed crest maxima compared with the second order theory, Eq. (10), for different values of sea state steepness, S_p.

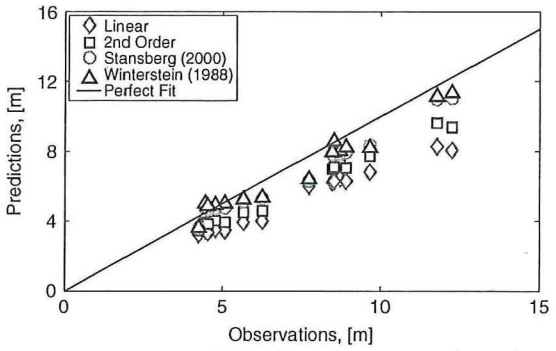

Fig. 5. Abnormal wave crests in the offshore basin versus the theory: (a) linear model – second order model; (b) second order model – modified second order model of Stansberg; (c) second order model – modified second order model of Winterstein.

sea states are represented by steepness at a step of approximately 0.02: $S_p \approx 0.022$, 0.045 and 0.058. Fig. 4 illustrates the theoretical results using the Hermite transformation model, designated by full signs and the observed values, designated by open signs. It is seen that the steeper sea state is associated with higher observed crests. The calculated percentage increase between the sea states represented by $H_s = 3.5$ m and $H_s = 7$ m is on the average 140%; the increase between the sea states represented by $H_s = 7$ m and $H_s = 9$ m is on the average 28%. The figure also shows larger scatter in the observed data for the steeper seas.

So far, the maximum crests in the records have been considered. Subsequently, applying the crest and height abnormality criteria, $CI > 1.3$ and $AI > 2$, and additionally requiring that the abnormality index AI is larger than 2 for both down-crossing and up-crossing waves, as discussed by Guedes Soares et al. [19,20], 15 events have been identified as being genuine abnormal waves. The significant wave height used in the ratios is the mean of one third of the largest wave heights. Waves following the upper criteria appear in all sea states considered.

Fig. 5 shows the results from the comparisons with the theories for these events only. In this case, the second order model [46] fails to describe the highest crests correctly. However, the observations agree in almost all cases with the Stansberg's model [45] and the Hermite model [52]. The two largest observed crests belong to test 8219 – the severest sea state. The second order extremes represented by squares in the graph overpredict the linear extremes by 13% on the average. Further increase of 14% is due to the γ_4 correction accounted for in the Stansberg's model or, respectively, 18% increase is observed when the non-Gaussian extreme are estimated after Winterstein [52]. The results conform to the study of Haver [25], who showed 15%–20% larger crests in a 3-h record when only the coefficient of skewness is included as a correction to the Gaussian model; further increase by 5% when γ_4 is calculated to leading second order and additional 2% increase

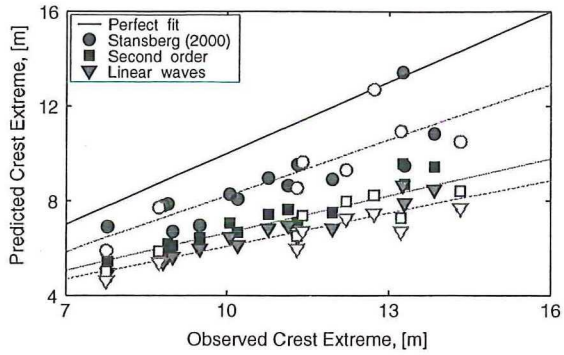

Fig. 6. Comparison between the observed maximum crests at North Alwyn and the predictions of the linear and second order based theories, including the modified second order model of Stansberg (according to Petrova et al. [40]).

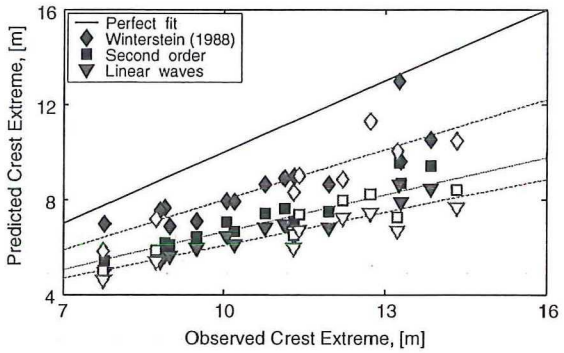

Fig. 7. Comparison between the observed maximum crests at North Alwyn and the predictions of the linear and second order based theories, including the modified second order model of Winterstein (according to Petrova et al. [40]).

when the third order contribution to γ_4 is considered in the calculations.

The results in Fig. 5 are not consistent with those reported earlier by Petrova et al. [40], which were based on full-scale data from the North Alwyn platform in the northern North Sea. The storm data represented 20-min records of the surface elevation sampled at frequency of 5 Hz. From the available 421 records, 23 waves have been identified as being abnormal considering the criterion $CI > 1.3$ and eight of them were subsequently classified as genuine freak waves, assuming that $CI > 1.3$ and $AI > 2$ for both down-crossing and up-crossing wave definitions. The comparison between the observed largest wave crests and the considered second order theoretical models validated the conclusion that the nonlinear characteristics of the sea states with abnormally high wave could not be described well by the models.

The comparisons with the theoretical models for North Alwyn are shown in Figs. 6 and 7. The open signs designate the genuine freak waves, while the full signs show the abnormal waves with only $CI > 1.3$. The tendency that the crests of the abnormal waves are constantly underestimated by the theoretical models could be due to the fact that the abnormal waves from the North Alwyn storm have higher nonlinearity. This is reflected in the larger skewness, as compared to the skewness estimates from the offshore basin. Only two cases of the full-scale extreme waves agree with Stansberg's model, as can be seen in Fig. 6. The predictions of the Hermite model fit well only one case (Fig. 7), which has been already well predicted by the model of Stansberg (Fig. 6).

The plots in Figs. 6 and 7, although illustrating larger discrepancies from the 'Perfect fit', in comparison with the laboratory waves (Fig. 5), follow the trend of increasing discrepancies from the modified second order models of Stansberg [45] and Winterstein [52] to the second order model and the linear model.

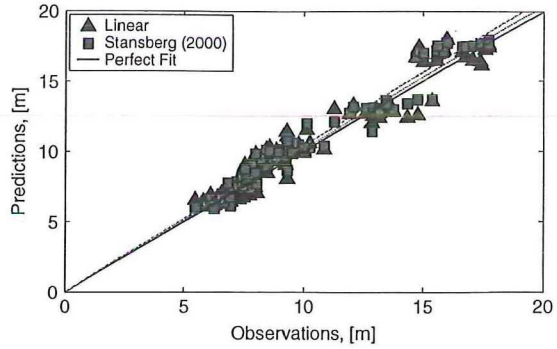

Fig. 8. The maximum wave heights from the offshore basin compared with the theoretical predictions of the linear model and the model of Stansberg.

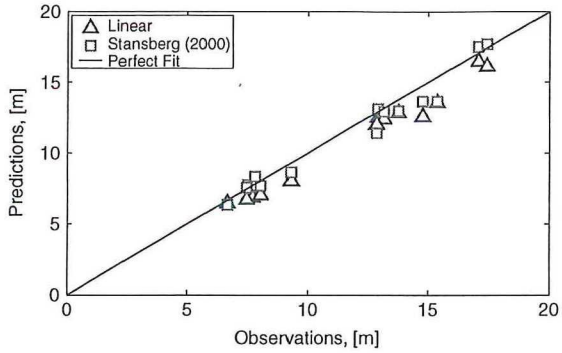

Fig. 9. The maximum wave height from the sea states with abnormal waves at the offshore basin compared with the linear predictions and the model of Stansberg.

Next, the largest wave heights are considered. Comparisons with the theoretical models for the highest waves at all gauges for a certain test are given in Fig. 8 and for the abnormal waves only are shown in Fig. 9. The solid line in the figures again describes the expected perfect agreement between observations and theory. The linear predictions are depicted by triangles and the predictions of the model of Stansberg — by squares. Fig. 8 shows that the extreme heights are well described by the linear equivalents for the majority of cases. The Stansberg's formula slightly overestimates the highest observations. However, it can be considered as the better fit to the abnormal cases shown in Fig. 9.

The results presented in Fig. 9 agree well with the results for storm sea [40]. It has been concluded that the model of Stansberg [45] serves as a reasonable fit to the abnormal wave heights from the considered storm at the North Alwyn platform, although most of the waves remained slightly underestimated. These results are shown for consistency in Fig. 10. Few waves have been slightly overestimated by the modified model. Two extremely large waves exceeding 17 m height have been also registered. They correspond to the cases of the largest predicted wave crests in Figs. 6 and 7.

The tendency that the waves generated in the basin are better approximated by the second order model [45] with empirically introduced correction by means of γ_4, could be related to the larger values of γ_4 observed in the tank. Different studies on the abnormal wave phenomenon have shown the strong correlation between the coefficient of kurtosis and the probability of occurrence of extremely high waves (e.g. [34] for laboratory waves; [19] for storm sea).

The presence of non-zero higher-order normalized cumulants can be used as a convenient measure for the deviation from the Gaussian surface. In contrast to the higher order statistical moments, which can take also non-zero values, for a Gaussian process all cumulant coefficients of order higher than second are

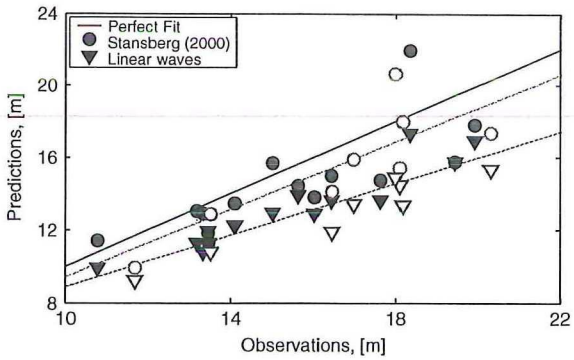

Fig. 10. Comparison between the observed maximum wave heights at North Alwyn and the predictions of the linear and the modified second order theory of Stansberg (according to Petrova et al. [40]).

equal to zero. The coefficient of skewness, γ_3, and the coefficient of kurtosis, γ_4, predicted by the second order theory are further compared with the estimates from the time series.

For a second order process, Vinje and Haver [50] derived a linear dependence between γ_3 and the significant wave steepness of the form:

$$\gamma_3 = 5.41 S_p. \tag{11}$$

However, it is based on the broad-banded Pierson–Moskowitz spectrum, which can result in higher estimate of the skewness. As the broader spectrum increases the nonlinearity of wave crests in deep water, Jha and Winterstein [26] proposed expressions for the statistics γ_3 and γ_4, which account for the spectral bandwidth trough the peakedness factor γ and the effect of finite water depth d:

$$\gamma_3 = 5.45\gamma^{-0.084} S_p + \left\{ \exp\left[7.41 \left(\frac{d}{L_p} \right)^{1.33} \right] - 1 \right\}^{-1} S_p. \tag{12}$$

The tank waves were generated from a JONSWAP spectrum with $\gamma = 3$. Furthermore, the depth effect in the present case is negligible, as far as the waves are propagating on deep-water.

Fig. 11 shows the comparison between the predicted and observed skewness, γ_3, plotted versus the significant steepness, S_p. The linear dependence [50], designated by VH in the figure, is shown by the dashed line and the linear trend of the calculated predictions following Eq. (12), designated by JW, is depicted by the thick line. It is seen that the models produce close results. The JW model predicts reasonably well the statistics of the sea states with $S_p > 0.04$, especially the statistics of the lowest sea state in that range of steepness, designated by 8241 ($H_s = 3.5$ m; $T_p = 7$ s). However, the observed skewness is overestimated for sea state 8201 with the minimum steepness values. As regards the abnormal wave statistics, the graph shows agreement with the JW model for most of the cases, which are plotted with full circles. Furthermore, it can be concluded that the results for the modelled waves do not depend on the severity of the sea state.

The abnormal waves associated with the North Alwyn storm [39] are also included in Fig. 11 and are designated by full triangles. Their statistics differ significantly from the statistics of the laboratory data, as it can be seen. The wind wave skewness falls above the predictions, contrary to the tendency observed for the tank data. Also, the maximum values of γ_3 exceed almost twice the values of γ_3 of the steepest abnormal waves in the offshore basin. The larger sampling scatter for the North Alwyn data is expected, since the time series are only 20-min long, as compared to the 3-h duration of the tank records. The observations from all unimodal seas are in relative agreement with the predictions of JW model, especially those from the seas with abnormal waves found.

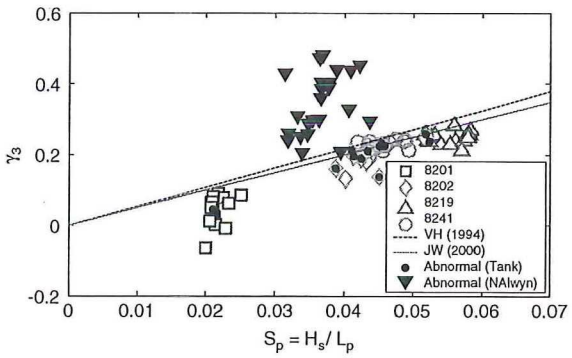

Fig. 11. S_p versus γ_3 for the unimodal sea states at the offshore basin and the sea states with abnormal waves at North Alwyn.

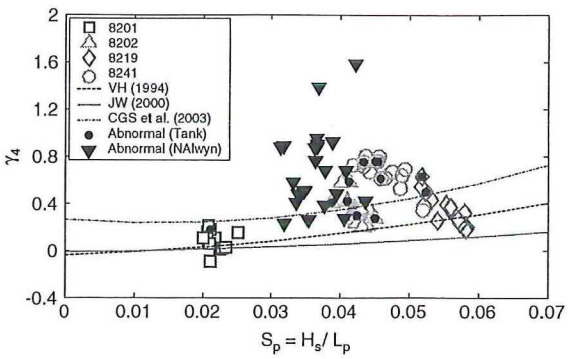

Fig. 13. S_p versus γ_4 for the unimodal sea states at the offshore basin and the sea states with abnormal waves at North Alwyn.

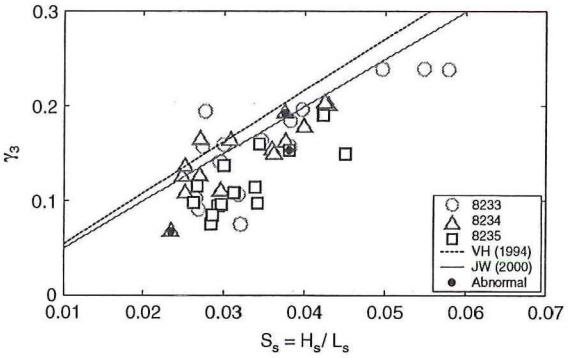

Fig. 12. S_s versus γ_3 for the bimodal sea states at the offshore basin.

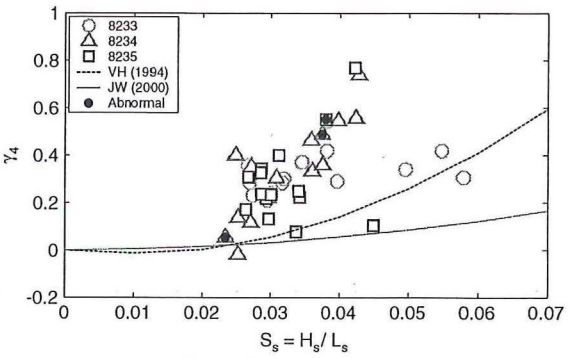

Fig. 14. S_s versus γ_4 for the bimodal sea states at the offshore basin.

The results for the two-peaked sea states registered at the tank are shown in Fig. 12. However, using the peak period in the definition of the sea state steepness is not the best option in this case, due to the bimodal shape of the spectra. Instead, the sea state steepness, designated by S_s in Fig. 12, has been recalculated on the basis of the significant wave period, i.e the mean period of the largest one third wave events in the records. Subsequently S_s has been used in the corresponding expressions for the coefficient of skewness and kurtosis, Eqs. (11) and (12).

It is seen that, contrary to the unimodal seas in Fig. 11, the two-peaked data cannot be distinguished in the figure, since they fall in the same range of values for S_s. The only exception is the test designated by 8233, which shows few significantly larger values, corresponding to the first three gauges in the basin. The large values here are reasonable, since this is the sea state where the two wave systems propagate at an angle of 60° and the spectra at the beginning of the tank have a negligible contribution from the low-frequency component. Moreover, the energy of the lower peak is less than 15% of the energy of the dominant peak, as required by Guedes Soares and Nolasco [22], in order to consider the lower peak as real. The data in Fig. 12 are more scattered than the one-peak data. The best fit is found for test 8234 (120°), while test 8235 (90°) is overestimated by both models. The good results for test 8234 could be explained with the strong effect of the swell component.

The three cases of genuine freak waves are shown in Fig. 12 with full circles. It is seen that the considered models predict larger values with one exception.

Fig. 13 represents a scatter plot between S_p and γ_4 for the cases of unimodal seas. The coefficient of kurtosis has been derived using the two quadratic dependencies: $\gamma_4 = 3(\gamma_3^2)$ [50], where some third order contribution to the coefficient of kurtosis is also taken into account, and $\gamma_4 = (1.41\gamma^{-0.02})\gamma_3^2$ [26]. It is seen that the two models tend to underpredict the kurtosis of the largest waves in the basin. However, good agreement is observed between the VH model and the data from tests 8201 and 8219. The corresponding calculations fall within approximately 1.5 standard deviations from the mean observed values. The biggest deviation from the models is found for the lowest sea – 8241, contrary to the results shown for the γ_3 statistics, when the data from test 8241 agree almost perfectly with the JW model and also with the VH model (Fig. 11).

Furthermore, significant underestimation is seen for the statistics of the abnormal extremes. This result confirms the conclusion of Jha and Winterstein [26] that the adequate prediction of γ_4 needs higher order effects, which are omitted in the second order model.

The γ_4 statistics of the abnormal extremes at North Alwyn plotted versus S_p in Fig. 13 show broader range of values in comparison with the values obtained in the tank, which can be also related to the sampling variability in the shorter storm records. The dash-dot line in Fig. 13 represents the relationship between γ_3 and γ_4 obtained by Guedes Soares et al. [19]. It is clear that that neither the expression of Vinje and Haver [50], nor the one of Jha and Winterstein [26] can give a reliable description of the considered storm data. Two considerably large values of γ_4 are also seen in Fig. 13; the largest corresponds to one of the biggest predicted wave crest and height in Figs. 6 and 7 and Fig. 10. However, on the basis of Fig. 11, it can be concluded that the observed difference between the waves in the open sea and the laboratory waves could be attributed to the specifics of these two types of situations. It is evident that the behaviour of the laboratory data does not depend on the sea state conditions, such as wind and current that may be present in the open sea.

The results for the extremes in the bimodal generated sea states are plotted in Fig. 14, using the sea steepness S_s. The tendency of underprediction of γ_4, which has been reported for the unimodal seas (Fig. 13) is also seen here. Again, it could be commented that

the models fail to predict the coefficient of kurtosis associated with the abnormal waves.

It must be noted that the results for the bimodal seas cannot be considered definite, since the models used are developed for unimodal spectra. Hence, further investigations are necessary regarding the statistics of combined sea.

4. Conclusions

The second order model and its modifications considered here give similar predictions for the maximum crest heights in the offshore basin. However, the γ_4 correction improves the statistical estimates. The waves, defined as abnormal are underestimated by the second order model of Tayfun [46], but they agree well with the Hermite transformation model of Winterstein [52].

The maximum wave heights are found to be in agreement with the linear assumption, $H = 2A$. However, the model of Stansberg is found to fit better the abnormal wave heights of the tank data.

Two functional dependencies for the coefficients of skewness and kurtosis, based on the second order wave theory, have been applied. The comparisons for γ_3 show better results for the model of Jha and Winterstein [26], which includes the effects of spectral bandwidth and finite water depth. The latter should not play a significant role for the tank waves, since they are propagating on deep water. Furthermore, the majority of the abnormal events match the line representing the JW model.

Larger deviation is found between the predictions of the second order theories and the observed values of γ_4. The models tend to underestimate the observations, especially the statistics of the abnormal wave events. However, good agreement is observed for some unimodal sea states.

Comparison between the results for the laboratory generated waves and the storm waves shows different statistical behaviour. In particular, the second order theories failed to predict the abnormal wave crests in the full-scale data. Furthermore, the associated coefficients of skewness are found to be underestimated by the proposed models, contrary to the result for the tank data. However, the results for the coefficient of kurtosis show that in both cases the models underestimate the observed statistics, particularly the statistics associated with the abnormal wave events.

The study on the statistics of the bimodal seas required recalculation of the sea steepness, S_p, since the peak frequency depends on the shape of the spectrum. Subsequently, the steepness based on the significant wave period has been chosen as representative for these sea states. The bimodal data demonstrated larger scatter. Furthermore, they tend to be overestimated by the models, contrary to the unimodal data, which are generally well predicted. As regards the coefficient of kurtosis, the observations are significantly higher than the model predictions.

Acknowledgements

This paper is an extended version of the presentation made at the 3rd Int. Workshop on Applied Offshore Hydrodynamics, held in Rio de Janeiro, Brazil, 17-19 October 2007.

The work has been performed in the scope of the project MARSTRUCT, Network of Excellence on Marine Structures (http://www.mar.ist.utl.pt/marstruct/), which has been financed by the EU through the GROWTH Programme under contract TNE3-CT-2003-506141. The data analysed in this paper has been obtained at MARINTEK in the scope of the project: Large Scale Facilities "Interactions Between Waves and Currents", which has been partially funded by the European Union under contract ERBFMGECT980135. The first author has been financed by the Portuguese Foundation of Science and Technology (FCT) under the grant SFRH/BD/30109/2006.

References

[1] Al-Humoud J, Tayfun A, Askar H. Distribution of nonlinear wave crests. Ocean Engineering 2002;29:1929–43.
[2] Antão E, Guedes Soares C. On the occurrence of abnormal waves in an offshore tank. Journal of Offshore Mechanics and Arctic Engineering 2008;130: 021008-1–021008-8.
[3] Arena F, Fedele F. A family of narrow-band non-linear stochastic processes for the mechanics of sea waves. European Journal of Mechanics – B/Fluids 2002; 21(1):121–37.
[4] Bateman W, Swan C, Taylor P. Steep multi-directional waves on constant depth. In: Proceedings of 18th International conference on offshore mechanics and arctic engineering. 1999. Paper OMAE99-6463.
[5] Bendat J, Piersol A. Random data: Analysis and measurement procedures. New York: John Wiley & Sons; 1971.
[6] Bitner-Gregersen E. Sea state duration and probability of occurrence of a freak crest. In: Proceedings of the 22nd international offshore mechanics and arctic engineering conference. 2003. Paper OMAE2003-37318.
[7] Bitner-Gregersen E, Hagen Ø. Freak wave events within the second order wave model. In: Proceedings of the 23rd international conference on offshore mechanics and arctic engineering. 2004.
[8] Boccotti P. On mechanics of irregular gravity waves. In: Atti Acc. Naz. Lincei. Memorie, vol. VIII. 1989. p. 11–170.
[9] Chien H, Kao C-C, Chuang L. On the characteristics of observed coastal freak waves. Coastal Engineering Journal 2002;44:301–19.
[10] Clauss G. Dramas of the sea: Episodic waves and their impact on offshore structures. Applied Ocean Research 2002;24:147–61.
[11] Dean R. Abnormal waves: A possible explanation. In: Torum A, Gudmestat O, editors. Water wave kinematics. Kluwer; 1990. p. 609–12.
[12] Donelan M, Magnusson A. The role of meteorological focusing in generating rogue wave conditions. In: Proceedings of the 14th winter workshop 'Aha Huliko'. 2005.
[13] Faulkner D, Buckley W. Critical survival conditions for ship design. In: Proceedings of the 1st international conference on design and operation for abnormal conditions. London (UK): RINA; 1997. p. 1–25. Paper no. 6.
[14] Fedele F, Arena F. Weakly nonlinear statistics of high random waves. Physics of Fluids 2005;17:1–10. Paper no. 026601.
[15] Fedele F, Tayfun A. Extreme waves and stochastic wave groups. In: Proceedings of the 25th international conference on offshore mechanics and arctic engineering. 2006. Paper OMAE2006-92527.
[16] Fonseca N, Guedes Soares C, Pascoal R. Prediction of ship dynamic loads in ship in heavy weather. In: Proceedings of the conference on design and operation for abnormal conditions II. London (UK): RINA; 2001. p. 169–82.
[17] Forristall G. Wave crest distributions: Observations and second order theory. Journal of Physical Oceanography 2000;30:1931–43.
[18] Guedes Soares C. Representation of double-peaked sea wave spectra. Ocean Engineering 1984;11(2):185–207.
[19] Guedes Soares C, Cherneva Z, Antão E. Characteristics of abnormal waves in North Sea storm sea states. Applied Ocean Research 2003;25:337–44.
[20] Guedes Soares C, Cherneva Z, Antão E. Abnormal waves during hurricane camille. Journal of Geophysical Research 2004;109: doi:10.1029/2003JC002244. C08008.
[21] Guedes Soares C, Fonseca N, Pascoal R, Clauss G, Schmittner C, Hennig J. Analysis of design wave loads on a FPSO accounting for abnormal waves. Journal of Offshore Mechanics and Arctic Engineering 2006;128:241–7.
[22] Guedes Soares C, Nolasco M. Spectral modelling of sea states with multiple wave systems. Journal of Offshore Mechanics and Arctic Engineering 1992; 114:278–84.
[23] Gumbel E. Statistics of extremes. NY (USA): Columbia University Press; 1958.
[24] Haver S, Andersen O. Freak waves – Myth or reality? In: Report OOS97*15547. STATOIL, Trondheim, Norway; 2000.
[25] Haver S. Design of offshore structures: Impact of the possible existence of freak waves. In: Proceedings of the 14th winter workshop 'Aha Huliko'. 2005.
[26] Jha A, Winterstein S. Nonlinear random ocean waves: Prediction and comparison with data. In: Proceedings of the ETCE/OMAE2000 joint conference energy for the new millennium. USA: ASME; 2000. Paper ETCE/OMAE2000-6125.
[27] Kharif C, Pelinovsky E. Physical mechanisms of the rogue wave phenomenon. European Journal of Mechanics, B/Fluids 2003;22:603–34.
[28] Krogstad H, Barstow S. Analysis and application of second order models for maximum crest height. In: Proceedings of the 21st international conference on offshore mechanics and arctic engineering. USA: ASME; 2002. Paper OMAE2002-28479.
[29] Marthinsen T, Winterstein S. On the skewness of random surface waves. In: Proceedings of the 2nd international offshore and polar engineering conference. 1992. p. 472–8.
[30] Mori N. Occurrence probability of a freak wave in a nonlinear wave field. Ocean Engineering 2004;31:165–75.
[31] Mori N. Effects of wave breaking on wave statistics for deep-water random wave train. Ocean Engineering 2003;30:205–20.
[32] Mori N, Yasuda T. Effects of high order nonlinear interactions on unidirectional wave trains. Ocean Engineering 2002;29:1233–45.
[33] Mori N, Liu P, Yasuda N. Analysis of freak wave measurements in the sea of Japan. Ocean Engineering 2002;29:1399–414.
[34] Mori N, Janssen P. On kurtosis and occurrence probability of freak waves. Journal of Physical Oceanography 2006;36:1471–83.
[35] Naess A. On the distribution of crest-to-trough wave heights. Ocean Engineering 1985;12(3):221–34.

[36] Onorato M, Osborne A, Serio M. On deviations from Gaussian statistics for surface gravity waves. In: Proceedings of the 14th winter workshop 'Aha Huliko'. 2005.
[37] Osborne A. Nonlinear instability analysis of deep water wave trains: Computation of maximum heights of rogue waves. In: Proceedings of the 19th international offshore mechanics and arctic engineering. ASME; 2000. Paper OSU OFT – 4033.
[38] Petrova P, Guedes Soares C. Spatial variability of the wave field generated in an offshore basin. In: Proceedings of the 9th international conference on stability of ships and ocean vehicles (STAB2006). Neves M, editor. COPPE, Rio de Janeiro, 2006. p. 287–98.
[39] Petrova P, Cherneva Z, Guedes Soares C. Distribution of crest heights in sea states with abnormal waves. Applied Ocean Research 2006;28:235–45.
[40] Petrova P, Cherneva Z, Guedes Soares C. On the adequacy of second-order models to predict abnormal waves. Ocean Engineering 2007;34:956–61.
[41] Sand S, Ottesen-Hansen N, Klinting P, Gudmestad O, Sterndoff M. Freak wave kinematics. In: Torum A, Gudmestad O, editors. Water wave kinematics. Dordrecht, The Nederlands: Kluwer Academic Publishers; 1990. p. 535–49.
[42] Skourup J, Andersen K, Hansen N. Non-Gaussian extreme waves in the central north Sea. In: Proceedings of the 13th international conference on offshore mechanics and arctic engineering. New York: ASME; 1996. p. 25–32.
[43] Stansberg C. Extreme waves in laboratory generated irregular wave trains. In: Tørum A, Gudmestad O, editors. Water wave kinematics. Kluwer Academic Publ.; 1990. p. 573–90.
[44] Stansberg C. Non-Gaussian extremes in numerically generated second-order random waves on deep water. In: Proceedings of the 8th international offshore and polar engineering conference. 1998. p. 103–10.
[45] Stansberg C. Random waves in the laboratory – What is expected for the extremes. In: Proceedings of the conference 'rogue waves', Ifremer, 2000, p. 289–301.
[46] Tayfun A. Narrow-band nonlinear sea waves. Journal of Geophysical Research 1980;85(C3):1548–52.
[47] Tayfun A, Fedele F. Wave-height distributions and nonlinear effects. Ocean Engineering 2007;34:1631–49.
[48] Tomita H, Kawamura T. Statistical analysis and inference from the in-situ data of the Sea of Japan with reference to abnormal or freak waves. In: Proceedings of the 10th international offshore and polar engineering conference. 2000. p. 116–22.
[49] Trulsen K, Dysthe K. Water wave kinematics computed with nonlinear Shrödinger theory. In: Proceedings of the 16th international offshore mechanics and arctic engineering conference. New York: ASME; 1997. p. 7–18.
[50] Vinje T, Haver S. On the non-Gaussian structure of ocean waves. In: Proceedings of the 7th conference 'behaviour of offshore structures'. Cambridge (USA): MIT; 1994.
[51] White B, Fronberg B. On the chance of freak waves at sea. Journal of Fluid Mechanics 1998;335:113–38.
[52] Winterstein S. Non-linear vibration models for extremes and fatigue. Journal of Fluid Mechanics 1988;114:1772–90.